Charging current: basics, compensation approximations, errors, and remediation

Tirath Bains, Ilia Voloh, Jc Theron, *GE Grid Solutions, Canada*
and Hebert Marchi Magalhaes , *ReEnergisa, Brazil*

Abstract—This paper idea was triggered by the line current differential misoperation due to incorrect charging current compensation settings. Authors investigated this case and concluded that this topic deserves better education on how and when to apply settings, because it's not straight forward to apply compensation with a shunt reactors providing different degree of the compensation and also which can be switched in or out. Topic becomes even more important with a longer underground and undersea cables, causing very high charging current.

Charging current compensation in long transmission lines and cables has been a standard practice for line differential elements. The relays usually estimate charging current is using positive and zero-sequence shunt reactance values provided by the user. However, the positive and zero-sequence shunt reactance are sufficient to accurately estimate the charging current only if a transmission line is fully transposed, thus, resulting in a diagonal sequence shunt impedance matrix. However, this assumption introduces an error in the charging current compensation. This paper investigates the charging current compensation with various sources of error engineers are not aware of and proposing remedial actions.

Firstly, this paper presents the theory and the formulae used to calculate the self and mutual capacitances of the transmission lines. Secondly, the assumptions involved to simplify the capacitance matrix such as fully transposed and symmetrical transmission lines are presented and discussed in detail. Then the paper analytically quantifies the amount of error expected in charging current compensation due to the above assumptions. Thereafter, the paper proposes the counter measures that could be taken to minimize the error in charging current compensation or to mitigate the effects of charging current compensation on the line differential and other protection elements. Various configurations of the transmission lines and cables are modelled in PSCAD, and the analytically estimated charging current is compared to the actual charging current of the un-transposed lines. Lastly, paper provides practical recommendations on in which applications charging current has to be enabled, it's not always needed.

Index Terms—Capacitance, charging current, line current differential, protection and control, transmission lines.

1 INTRODUCTION

THE existence of shunt capacitance between phase-to-phase and phase-to-ground in transmission lines and cables leads to the charging current. As the level of system voltage become higher and the length of the lines increases, the phenomenon of charging current becomes more and more pronounced. This charging current is observed as differential current by the line current differential element (87L). If the charging current is significant then its compensation is required to maintain the security and the sensitivity of the 87L element. A field case was encountered recently where 87L mal-operated due to incorrect application of charging current compensation. This highlights the fact that it is very important for the protection engineers to have knowledge about estimating charging current, various methods used by relays to compensate charging current and how to properly apply charging current compensation. This paper aims to discuss various aspects of the theory and modeling of the shunt capacitance, the resulting charging current, issues arising due to charging current and various methods of remediation.

The Section 2 presents the theory behind the phenomenon of shunt capacitance, how it can be estimated analytically using conductor arrangement data, and what are the impacts of transposition on capacitance in phase-domain and sequence domain. Section 3 presents the method for calculating the charging current from the estimated line capacitance values. Various methods for compensating charging current are discussed in Section 4. Section 5 describes the test system simulated in PSCAD which is utilized to support the analytical findings and elaborate on the application of charging current compensation. Section 6 discusses various scenarios when and how to apply charging current compensation. A detailed analysis of an actual field case where mal-operation of 87L element occurred due to erroneous application of charging current compensation in Section 7. Section 8 lists the various recommendations about the application of the charging current compensation. The conclusion is provided in Section 9.

2 SHUNT CAPACITANCE

In order to understand the phenomenon of charging current, it is necessary to understand the origins of shunt capacitance. Figure 1 shows a cylindrical conductor of length l metres and radius r metres carrying the charge per unit length $q\ \frac{C}{m}$. By applying Gauss's law it can be proved that the electric field intensity (E) at any given point which is x ($x > r$) meters away from the cylindrical conductor is given by:

$$E_x = \frac{q}{2\pi\epsilon_0 x} V/m \tag{1}$$

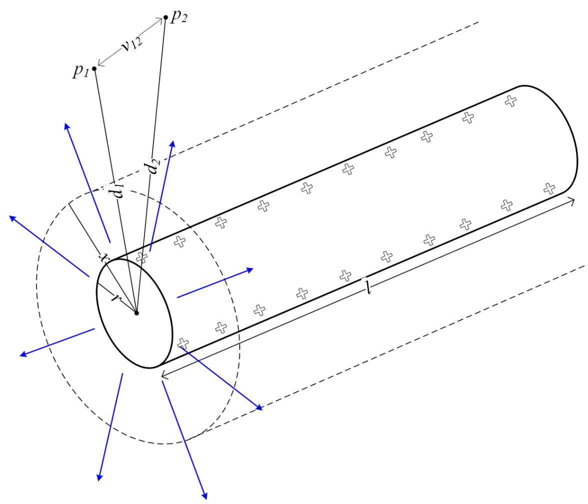

Fig. 1. Electric field due to a cylindrical charged conductor.

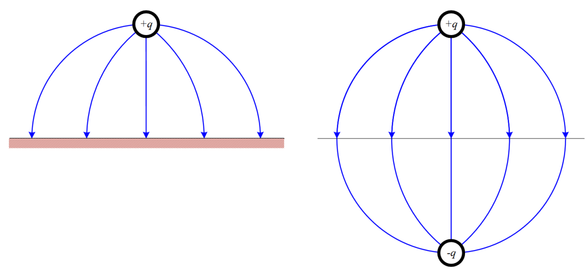

Fig. 2. Effect of earth on the electric field due to a cylindrical charged conductor.

where ϵ_0 is the permittivity of the free space with $\epsilon_0 = 8.854 \times 10^{-9} \frac{F}{km}$. The direction of the electric field lines will radiate out/in (if charge is positive/negatively, respectively) radially from the conductor. Based on equation (1) it can be seen that any concentric cylindrical surface of radius x will be equi-potential. The potential difference between two points $p1$ and $p2$ located at distance $d1$ and $d2$, respectively can be calculated by integrating the electric field intensity along the radial path from equi-potential surfaces of p1 and p2:

$$V_{12} = \int_{d1}^{d2} \frac{q}{2\pi\epsilon_0 x} dx = \frac{q}{2\pi\epsilon_0} \ln \frac{d2}{d1} \tag{2}$$

Another factor to consider is the presence of the earth. The earth changes the electric field due to the charged conductor, therefore earth needs to be accounted for. The earth is approximated as a perfect conducting surface [1], which makes the earth surface an equi-potential surface, thus, the electric filed lines will meet the surface of the earth perpendicularly as shown in Figure 2 (a). Now, the electric field due to the charge conductor can be assumed to converge at a virtual conductor which is the mirror image of the real conductor but with the opposite charge polarity as Figure 2 (b) shows. Thus, the effect of earth can be accounted for by assuming a mirror image of the actual charged conductors below the surface of the earth with equal charge but with opposite polarity.

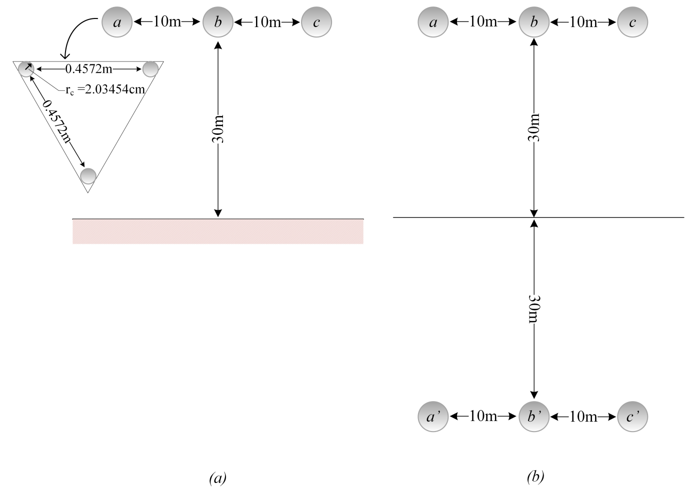

Fig. 3. A three phase conductor arrangement on a tower: (a) over the earth surface plane, (b) earth replaced by a perfect conducting surface plane showing mirrored conductors.

2.1 Calculating shunt capacitance: 3-phase line

Consider a three phase line with the following dimensions given in the Figure 3, which is one of the typical arrangements for a $500kV$ transmission line. It should be noted that for this example, a bundle of 3 conductors per phase is used. The effective radius of a conductor or a bundle of conductors is as given below:

- for one-conductor bundle: $r = r_c$
- for two-conductor bundle: $r = \sqrt{r_c d}$
- for three-conductor bundle: $r = \sqrt[3]{r_c d^2}$
- for four-conductor bundle: $r = \sqrt[4]{r_c d^3}$

were d is the distance between the conductors within a bundle, r_c is the radius of the conductor. For the transmission line shown in Figure 3, $r_c = 0.0203454m$ while $d = 0.4572cm$.

The equivalent circuit by replacing the earth with image conductors is shown in the Figure 3 (b). Now using the equation (2), the expression for the potential difference between phase-A conductor and its image,i.e., $V_{aa'}$ can be written as:

$$\begin{aligned} V_{aa'} &= \frac{1}{2\pi\epsilon_0}[q_a \ln\frac{D_{a'a}}{r} + q_b \ln\frac{D_{a'b}}{D_{ab}} + q_c \ln\frac{D_{a'c}}{D_{ac}} \\ &\quad -q_a \ln\frac{r}{D_{a'a}} + q_b \ln\frac{D_{ab}}{D_{a'b}} + q_c \ln\frac{D_{ac}}{D_{a'c}}]V \\ &= \frac{2}{2\pi\epsilon_0}[q_a \ln\frac{D_{aa'}}{r} + q_b \ln\frac{D_{a'b}}{D_{ab}} + q_c \ln\frac{D_{a'c}}{D_{ac}}]V \end{aligned} \tag{3}$$

Since $V_{an} = \frac{1}{2} V_{aa'}$,

$$V_{an} = \frac{1}{2\pi\epsilon_0}[q_a \ln\frac{D_{a'a}}{r} + q_b \ln\frac{D_{a'b}}{D_{ab}} + q_c \ln\frac{D_{a'c}}{D_{ac}}]V \tag{4}$$

Similar equations can be written afor V_{bc}, V_{ca}, thus resulting in the following matrix:

$$\begin{bmatrix} V_{an} \\ V_{bn} \\ V_{cn} \end{bmatrix} = \frac{1}{2\pi\epsilon_0} \begin{bmatrix} \ln\frac{D_{a'a}}{r} & \ln\frac{D_{a'b}}{D_{ab}} & \ln\frac{D_{a'c}}{D_{ac}} \\ \ln\frac{D_{b'a}}{D_{ba}} & \ln\frac{D_{b'b}}{r} & \ln\frac{D_{b'c}}{D_{bc}} \\ \ln\frac{D_{c'a}}{D_{ca}} & \ln\frac{D_{c'b}}{D_{cb}} & \ln\frac{D_{c'c}}{r} \end{bmatrix} \begin{bmatrix} q_a \\ q_b \\ q_c \end{bmatrix} \tag{5}$$

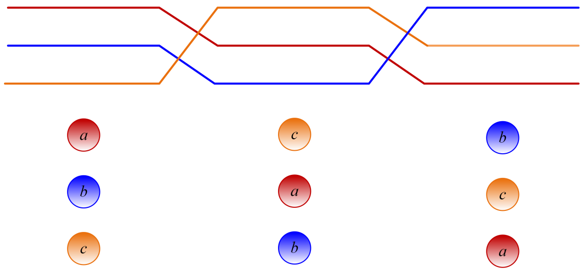

Fig. 4. Transposition of the transmission line.

Since, it is a known fact that $[q] = [C_p][V]$ where $[C_p]$ is phase capacitance matrix. By looking at equation (5), it can be observed that $[C_p]$ can be obtained from the following expression:

$$\begin{bmatrix} C_{aa} & C_{ab} & C_{ac} \\ C_{ab} & C_{bb} & C_{bc} \\ C_{ac} & C_{bc} & C_{cc} \end{bmatrix} = \begin{bmatrix} \frac{1}{2\pi\epsilon_0} \begin{bmatrix} \ln\frac{D_{a'a}}{r} & \ln\frac{D_{a'b}}{D_{ab}} & \ln\frac{D_{a'c}}{D_{ac}} \\ \ln\frac{D_{b'a}}{D_{ba}} & \ln\frac{D_{b'b}}{r} & \ln\frac{D_{b'c}}{D_{bc}} \\ \ln\frac{D_{c'a}}{D_{ca}} & \ln\frac{D_{c'b}}{D_{cb}} & \ln\frac{D_{c'c}}{r} \end{bmatrix} \end{bmatrix}^{-1} \quad (6)$$

Substituting the distance values from Figure 3(b) in equation (6) and computing, following is obtained:

$$\begin{bmatrix} C_{aa} & C_{ab} & C_{ac} \\ C_{ab} & C_{bb} & C_{bc} \\ C_{ac} & C_{bc} & C_{cc} \end{bmatrix} = \begin{bmatrix} 1.0490 & -0.2840 & -0.1173 \\ -0.2840 & 1.1128 & -0.1510 \\ -0.1173 & -0.2840 & 1.0490 \end{bmatrix} \times 10^{-8} \frac{F}{km} \quad (7)$$

It can be seen from equation (7) that $C_{ab} = C_{bc} \neq C_{ac}$ and $C_{aa} = C_{cc} \neq C_{bb}$. This is logical and it happens due to the fact that the positions of phase-A and phase-C conductors are identical with respect to that of phase-B conductor, and also their positions are identical with respect to each other. It should be noted that conductor sag is neglected while deriving the values shown in (7). The effect of conductor sag on shunt capacitanes can be accounted for by lowering the effective height of the conductor in equation (6) as described in [2].

2.2 Transposition of Transmission Line

The arrangement of the conductors of the in a fully transposed line is as shown in Figure 4. In a fully transposed line any given phase will occupy a specific position for one-third of the line length, then will be replaced by the other phases sequentially. In this paper, the conductor arrangement considered so far has been *abc* arrangement. In order to derive the shunt capacitance for a fully transposed line, the equivalent of equation (6) could be written for the conductor arragements *abc*, *cab*, *bca*, and final matrix is consitututed by averaging the corresponding terms of these three combinations. Alternatively, the shunt capacitance for a fully transposed line line can also be calculated by replacing the terms D_{ab},D_{bc}, D_{ac} with the term $\sqrt[3]{D_{ab}D_{bc}D_{ca}}$; and replacing the terms $D_{a'b}$, $D_{b'c}$, $D_{a'c}$ with the term $\sqrt[3]{D_{a'b}D_{b'c}D_{c'a}}$ in (6). Both approaches are equivalent, and both will yield the following result:

$$\begin{bmatrix} C_{aa} & C_{ab} & C_{ac} \\ C_{ab} & C_{bb} & C_{bc} \\ C_{ac} & C_{bc} & C_{cc} \end{bmatrix} = \begin{bmatrix} 1.0596 & -0.2240 & -0.2240 \\ -0.2240 & 1.0596 & -0.2240 \\ -0.2240 & -0.2240 & 1.0596 \end{bmatrix} \times 10^{-8} \frac{F}{km} \quad (8)$$

2.3 Shunt capacitance in sequence domain

The shunt capacitance in sequence domain can be calculated using

$$\begin{bmatrix} C_{00} & C_{01} & C_{02} \\ C_{10} & C_{11} & C_{12} \\ C_{20} & C_{21} & C_{22} \end{bmatrix} = \frac{1}{3} \begin{bmatrix} 1 & 1 & 1 \\ 1 & \alpha^2 & \alpha \\ 1 & \alpha^2 & \alpha \end{bmatrix} \begin{bmatrix} C_{aa} & C_{ab} & C_{ac} \\ C_{ab} & C_{bb} & C_{bc} \\ C_{ac} & C_{bc} & C_{cc} \end{bmatrix} \begin{bmatrix} 1 & 1 & 1 \\ 1 & \alpha & \alpha^2 \\ 1 & \alpha^2 & \alpha \end{bmatrix} \quad (9)$$

where $\alpha = 1\angle 120^o$. Now substituting the phase shunt capacitance values from (8) in (9), the sequence shunt capacitance values are obtained as follows:

$$\begin{bmatrix} C_{00} & C_{01} & C_{02} \\ C_{10} & C_{11} & C_{12} \\ C_{20} & C_{21} & C_{22} \end{bmatrix} = \begin{bmatrix} 0.6116 & 0 & 0 \\ 0 & 1.2837 & 0 \\ 0 & 0 & 1.2837 \end{bmatrix} \times 10^{-8} \frac{F}{km} \quad (10)$$

Note that off-diagonal elements are Zero, which implies that capacitances in sequence domain are decouple from each other, i.e., changes in one sequence would not affect the other sequences. This due to the fact the transmission line is fully transposed. If the line is not fully transposed then the off-diagonal elements will be non-zero and complex, and as a result the sequence components will be coupled. The effects of non-transposition on estimating charging current are discussed later.

In the discussion so far was aimed at estimating line shunt capacitances through analytical approach. Another approach which is based on the using recorded current and voltage waveforms to estimate line shunt capacitance/reactances is presented in Appendix A [3].

3 Charging Current

It is known fact that the current through a capacitor is governed by the following equation:

$$i_C = C\frac{\partial v}{\partial t} \quad (11)$$

where v is the voltage across the capacitor,i_C represents the current through the capacitor, $\frac{\partial}{\partial t}$ represents the derivative with respect to time (t), C represents the capacitance of the capacitor. Similarly, for a three phase line the charging current can be calculated using the following relation:

$$\begin{bmatrix} i_{aC} \\ i_{bC} \\ i_{cC} \end{bmatrix} = \begin{bmatrix} C_s & C_m & C_m \\ C_m & C_s & C_m \\ C_m & C_m & C_s \end{bmatrix} \frac{\partial}{\partial t} \begin{bmatrix} v_a \\ v_b \\ v_c \end{bmatrix} \quad (12)$$

where C_s and C_m represent the self and mutual capacitances of the transmission line. v_a, v_b, v_c are the phase to ground voltages while i_{aC}, i_{bC}, i_{cC} are the charging currents in each phase. The assumption is that the line is fully transposed. It is worth noting here that C_m is a negative number, which is logical because when a positive voltage is applied to a phase it will induce negative charge on the other two phases.

In sequence-domain the charging current can be obtained as per the equation (13).

$$\begin{bmatrix} i_{0C} \\ i_{1C} \\ i_{2C} \end{bmatrix} = \begin{bmatrix} C_0 & 0 & 0 \\ 0 & C_1 & 0 \\ 0 & 0 & C_1 \end{bmatrix} \frac{\partial}{\partial t} \begin{bmatrix} v_0 \\ v_1 \\ v_2 \end{bmatrix} \quad (13)$$

where C_0 and C_1 represent zero-sequence capacitance and positive-sequence capacitance, respectively. v_0, v_1, v_2 represent the zero, positive, negative-sequence voltages, respectively; i_{0C}, i_{1C}, i_{2C} represent the zero, positive, negative-sequence charging currents, respectively. Now, the charging current in phase-domain domain can be obtained by using proper combination of sequence-domain charging currents. Both approaches, i.e., equation (12) and equation (13) are equivalent. However, since equation (12) yields the result directly in phase-domain, it is considered in this paper.

Now, the phase capacitance matrix of equation (12) can be expressed in terms of C_0 and C_1 as equation (3).

$$\begin{bmatrix} C_s & C_m & C_m \\ C_m & C_s & C_m \\ C_m & C_m & C_s \end{bmatrix} = \frac{1}{3}\begin{bmatrix} 1 & 1 & 1 \\ 1 & \alpha^2 & \alpha \\ 1 & \alpha & \alpha^2 \end{bmatrix}\begin{bmatrix} C_0 & 0 & 0 \\ 0 & C_1 & 0 \\ 0 & 0 & C_1 \end{bmatrix}\begin{bmatrix} 1 & 1 & 1 \\ 1 & \alpha & \alpha^2 \\ 1 & \alpha^2 & \alpha \end{bmatrix}$$

$$\Longrightarrow \begin{bmatrix} C_s & C_m & C_m \\ C_m & C_s & C_m \\ C_m & C_m & C_s \end{bmatrix} = \frac{1}{3}\begin{bmatrix} C_0+2C_1 & C_0-C_1 & C_0-C_1 \\ C_0-C_1 & C_0+2C_1 & C_0-C_1 \\ C_0-C_1 & C_0-C_1 & C_0+2C_1 \end{bmatrix} \quad (14)$$

Substituting the expression (3) in equation (12), the equation (15) is obtained which yields the phase charging current directly from sequence capacitance values.

$$\begin{bmatrix} i_{aC} \\ i_{bC} \\ i_{cC} \end{bmatrix} = \frac{1}{3}\begin{bmatrix} C_0+2C_1 & C_0-C_1 & C_0-C_1 \\ C_0-C_1 & C_0+2C_1 & C_0-C_1 \\ C_0-C_1 & C_0-C_1 & C_0+2C_1 \end{bmatrix} \frac{\partial}{\partial t}\begin{bmatrix} v_a \\ v_b \\ v_c \end{bmatrix} \quad (15)$$

Normally, the transmission line parameters that are more easily available are capacitive shunt reactances rather than shunt capacitances. Therefore the equation (15) is re-written in terms of zero-sequence reactance (X_{C0}) and positive-sequence reactance (X_{C1}) as equation (16).

$$\begin{bmatrix} i_{aC} \\ i_{bC} \\ i_{cC} \end{bmatrix} = \frac{1}{3\omega}\begin{bmatrix} \frac{1}{X_{C0}}+\frac{2}{X_{C1}} & \frac{1}{X_{C0}}-\frac{1}{X_{C1}} & \frac{1}{X_{C0}}-\frac{1}{X_{C1}} \\ \frac{1}{X_{C0}}-\frac{1}{X_{C1}} & \frac{1}{X_{C0}}+\frac{2}{X_{C1}} & \frac{1}{X_{C0}}-\frac{1}{X_{C1}} \\ \frac{1}{X_{C0}}-\frac{1}{X_{C1}} & \frac{1}{X_{C0}}-\frac{1}{X_{C1}} & \frac{1}{X_{C0}}+\frac{2}{X_{C1}} \end{bmatrix} \frac{\partial}{\partial t}\begin{bmatrix} v_a \\ v_b \\ v_c \end{bmatrix} \quad (16)$$

In phasor domain, the equation (16) becomes (17).

$$\begin{bmatrix} I_{aC} \\ I_{bC} \\ I_{cC} \end{bmatrix} = j\frac{1}{3}\begin{bmatrix} \frac{1}{X_{C0}}+\frac{2}{X_{C1}} & \frac{1}{X_{C0}}-\frac{1}{X_{C1}} & \frac{1}{X_{C0}}-\frac{1}{X_{C1}} \\ \frac{1}{X_{C0}}-\frac{1}{X_{C1}} & \frac{1}{X_{C0}}+\frac{2}{X_{C1}} & \frac{1}{X_{C0}}-\frac{1}{X_{C1}} \\ \frac{1}{X_{C0}}-\frac{1}{X_{C1}} & \frac{1}{X_{C0}}-\frac{1}{X_{C1}} & \frac{1}{X_{C0}}+\frac{2}{X_{C1}} \end{bmatrix}\begin{bmatrix} V_a \\ V_b \\ V_c \end{bmatrix} \quad (17)$$

where, I_{aC}, I_{bC}, I_{cC} represent the phasors of the charging current in phase-A, B, and C, respectively; V_a, V_b, V_c are the phasors of phase to ground voltage in phase-A, B, and C respectively; ω is the angular frequency of the system.

4 Methods of Mitigating the Effects of Charging Current on 87L

4.1 Higher cut-off for 87L

This method involves setting the minimum pickup value of 87L above the maximum charging current of the protected transmission line. Typically, setting the minimum pick-up level at 120% would offer a good security margin. This ensures that the differential current arising due to charging current would not force the operation of 87L. Raising the minimum pickup value of 87L is a straightforward approach, however, it desensitizes the 87L element to detect high impedance faults in the transmission line.

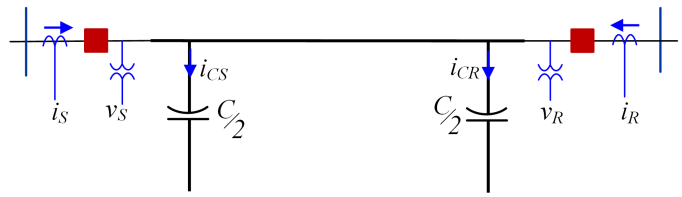

Fig. 5. Voltage-based charging current compensation in two-terminal transmission line.

4.2 Fixed charging current compensation

In this method, the charging current is estimated through calculations or through simulations, and then a fixed value of the estimated charging current is subtracted from the measured line currents. When system is operating at rated voltage level and under steady state conditions, this method would provide accurate charging current compensation. However, the system voltage could change by few percentage points and the fixed charging current compensation value does not remain accurate anymore. Moreover, the external faults/disturbances would result in significant difference between the actual charging current and the fixed charging current compensation. Therefore, the fixed charging current compensation might be needed to be blocked when it is needed the most, i.e., to safeguard the 87L operation for external faults. Due to the reasons discussed above the authors are not aware of the usage of this method.

4.3 Voltage measurement-based charging current compensation

If three phase voltages are available, the charging currents can be estimated by using the equation (15) in time domain or by using equation (17) in phasor-domain.

The disadvantage of compensation in phasor domain is that during an external fault the voltage phasor would reach its actual value from its pre-fault value only after the time period of a full-cycle (assuming full cycle DFT is used for phasor estimation) has elapsed. As a result the charging current compensation will not be correct for the duration of the phasor estimation delay. Therefore, the voltage-based charging current compensation presented from here onwards is based in time-domain.

In order to calculate the charging current in a two-ended transmission line half of the line capacitance is assumed to be lumped at each end of the transmission line as shown in Figure 5. Equation (18) shows the calculation of the charging current at sending end terminal S, where $[i_S]$ and $[i_{CS}]$ represent the measured current and the charging current matrices, respectively at Terminal S; $[v_S]$ is the measured voltage matrix at Terminal S; $[C]$ is the matrix of transmission line shunt capacitance. Note that a factor of $\frac{1}{2}$ appears in equation (18) when compared to equation (15), due to the fact that only half of the total capacitance is assumed to be lumped at sending end terminal. Now, $[i_{CS}]$ is then subtracted from $[i_S]$ to obtain compensated current matrix at Terminal S, i.e., $\left[i_S'\right]$ as shown in equation (19). Now, the current $\left[i_S'\right]$ is the current that participates in the calculation of the differential current.

$$[i_{CS}] = \frac{[C]}{2}\frac{\partial}{\partial t}[v_S] \tag{18}$$

$$[i_S^{'}] = [i_S] - \frac{[C]}{2}\frac{\partial}{\partial t}[v_S] \tag{19}$$

Similarly, the compensated current matrix at receiving end terminal R $\left[i_R^{'}\right]$ is calculated as per equation (20) where $[i_R]$ and $[v_R]$ represent the measured current and measured voltage matrices at Terminal R.

$$[i_R^{'}] = [i_R] - \frac{[C]}{2}\frac{\partial}{\partial t}[v_R] \tag{20}$$

Now the differential current as seen by the element 87L $[[i_{DIFF}]]$ is calculated as below:

$$\begin{aligned} [i_{DIFF}] =& [i_{DS}] + [i_{DR}] \\ \implies [i_{DIFF}] =& [i_S] + [i_R] - \frac{[C]}{2}\frac{\partial}{\partial t}[v_S] - \frac{[C]}{2}\frac{\partial}{\partial t}[v_R] \end{aligned} \tag{21}$$

It can be observed from equation (21) that when the compensated currents are used for calculating the differential current, the total charging current of the transmission gets deducted, resulting in a very small to negligible differential current. As a matter of fact that equation (21) can be easily adapted to N terminal transmission line. For transmission line with N terminals it is assumed that capacitance $\frac{[C]}{N}$ is lumped at each terminal, thus resulting in equation (22). Note that charging current for whole transmission line gets compensated when calculating differential current.

$$\begin{aligned} [i_{DIFF}] =& [i_S] + [i_R] + ... + [i_R] - \frac{[C]}{N}\frac{\partial}{\partial t}[v_S] \\ & - \frac{[C]}{N}\frac{\partial}{\partial t}[v_R] - ... - \frac{[C]}{N}\frac{\partial}{\partial t}[v_N] \end{aligned} \tag{22}$$

5 Test System

In order to elaborate the details of charging current compensation it is desirable to simulate a test system. A 500kV test system with transmission line having conductor arrangement shown in Figure 3 (a) is simulated in PSCAD. The transmission line length is varying from case to case basis, and is mentioned with each case. To simulate the transmission line, a frequency-dependent model of transmission line available in PSCAD is utilized. The line positive and zero-sequence impedances are $Z_{L1} = (0.0117 + j0.3341)$ Ω/km and $Z_{L0} = (0.1770 + j1.300)$ Ω/km, respectively. The line positive and zero-sequence admittances are $Y_{L1} = j4.8475 \times 10^{-6}$ S/km ($C_1 = 1.2858 \times 10^{-8}$ F/km), $Y_{L0} = j2.3075 \times 10^{-6}$ S/km ($C_0 = 0.6120 \times 10^{-8}$ F/km), respectively. Note that the zero-sequence and positive-sequence shunt capacitive values obtained from PSCAD closely match those calculated theoretically in equation (10). The sending end and receiving end sources are identical with positive and zero-sequence impedances being $Z_{S1} = Z_{R1} = (1 + j36)$ Ω and $Z_{S0} = Z_{R0} = (1.5 + j54)$ Ω, respectively. Load angle is 30° with receiving end source voltage lagging. Further, the current and voltage signals are obtained by using CT and CVT models, respectively, available in PSCAD. The CT ratio is 400 with CT Secondary of 5A, while CVT Ratio is 3000. It should be noted that units of the current waveforms in the subsequent figures are per unit of CT nominal value.

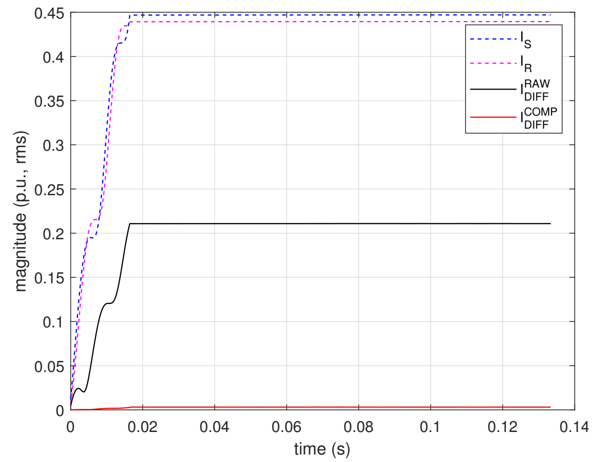

Fig. 6. Voltage-based charging current compensation in two-terminal fully transposed transmission line.

6 Cases for application of the charging current compensation

6.1 Long fully transposed transmission line

A 300km long fully transposed transmission was simulated in the test system described in Section 5 with a load angle of 30°. Figure 6 shows the sending (I_S) and receiving currents (I_R) along with 'fictitious' differential current (I_{DIFF}^{RAW}), which arises purely due to the steady state charging current of the transmission line. I_{DIFF}^{COMP}) represents the 'fictitious' differential current after the charging current compensation has been applied as per equation (21). It can be observed that, the magnitude of I_{DIFF}^{RAW} is higher than 0.2p.u. (400A). When charging current compensation is applied the 'fictitious' differential current drops almost to Zero. I_{DIFF}^{COMP} does have a small finite value due to the fact that *pi*-model of the transmission line loses some accuracy when the transmission line length is over 200km. As expected it can be observed that applying charging current compensation greatly increases the security band of 87L while enabling the much more sensitive settings.

6.2 Long fully untransposed transmission line

The transmission line of the previous case was made fully untransposed and the same loading conditions were applied. The charging current compensation is applied by assuming that line is fully transposed. The result is shown in Figure 7. It is seen that charging current compensation reduces the 'fictitious' differential significantly from about 0.2pu to about 0.02pu. However, as compared to the fully transposed case, this case has higher 'fictitious' differential current. This is due to the fact that for untransposed line, the sequence networks are coupled but the charging current compensation is applied assuming that the sequence networks are uncoupled. In order to achieve higher accuracy the off-diagonal elements of equation (10) which are non-zero for untransposed line would also be required, and which are usually not available. It should be noted that the line studied is a 300km line and the amount of charging current that could not be removed using zero and positive sequence capacitances alone is about 0.02pu (40A), which

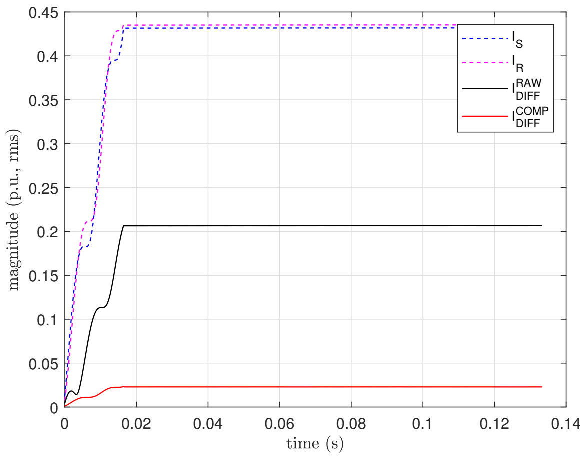

Fig. 7. Voltage-based charging current compensation in two-terminal fully untransposed transmission line.

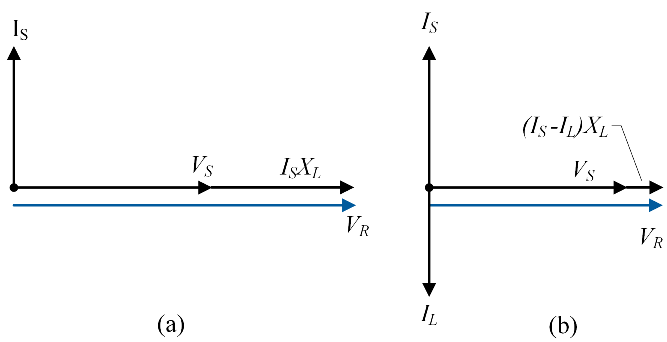

Fig. 8. Phasor diagram depicting: (a) Ferranti effect, (b) remediation through shunt reactors.

is significantly low enough to allow for sensitive settings of 87L. It can thus be concluded that charging current compensation in untransposed long transmission line will largely remove 'fictitious' differential current and should be applied.

6.3 Presence of shunt reactors

The shunt reactors are provided to prevent the over-voltage at the receiving end of the transmission line when it lightly or unloaded. The unloaded or lightly loaded long transmission line draws predominantly capacitive current from the sending end due to its shunt capacitance. The capacitive current causes voltage drop in transmission line which add constructively in the sending end voltage which causes causes the receiving end voltage to rise. This effect is called 'Ferranti effect'. which can be understood with the help of Figure 8(a) where V_S and V_R denote sending and receiving voltage phasors respectively; I_S is the current at sending end (capacitive in nature); X_L is the reactance of the transmission line. When a shunt reactor is added, the the capacitive current is compensated by the inductive current of the reactor, thus, leading to limited to no over-voltage at receiving end as shown in Figure 8(b).

Whereas the shunt reactors are useful in preventing over-voltage in lightly loaded long transmission lines, they require special attention when applying charging current compensation which is discussed as follows.

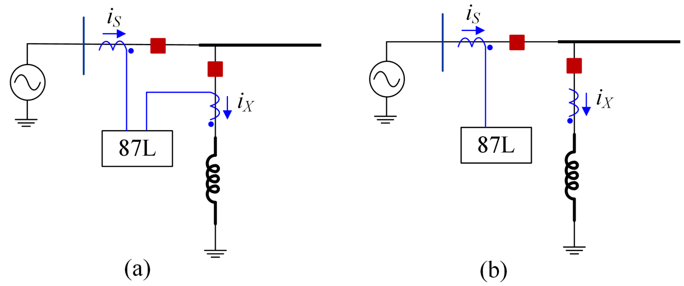

Fig. 9. Reactors connected to transmission line: (a) excluded from the protection (b) included in the protection Zone.

6.3.1 *Shunt reactors excluded in the protection zone*

Figure 9 (a) shows the shunt reactors excluded from the protection zone which is achieved by removing the reactor current from the measured current at the transmission line terminals. In this case, the charging current of the whole of the transmission line will appear as differential current. In order to compensate the charging current the positive and zero-sequence capacitive reactance of the transmission lines are needed to be entered only, irrespective of the reactance of the shunt reactors.

6.3.2 *Shunt reactors included in the protection zone*

The shunt reactors are included in the protection zone, when reactor current is not removed from the measured current at the transmission line terminals. When the shunt reactors are connected to the transmission line, the differential current due to charging current decreases because shunt reactors compensate the capacitive charging current of the line. However, the shunt reactors could also be entirely or partially disconnected from the transmission line depending upon the desired and actual voltage level. When the shunt reactors are disconnected entirely, the differential current would now be the charging current of the whole of transmission line. Therefore, when reactors are included in the protection zone then the charging current compensation would be required to change dynamically, depending upon the whether the shunt reactors are connected, disconnected or partially connected.

When shunt reactors are included in the protection zone, the shunt reactance used for calculating charging current would be the parallel combination of the shunt capacitance of the transmission line and reactance of the reactors. The effective capacitive reactance can be calculated as follows:

- Three reactor arrangement: In a three reactor arrangement the three reactors of equal reactance (X_R) are connected to each phase as shown in Figure 10 (a). As a result the positive and zero-sequence reactance of the reactor arrangement are equal, i.e., $X_{R1} = X_{R0} = X_R$. The equations for the effective

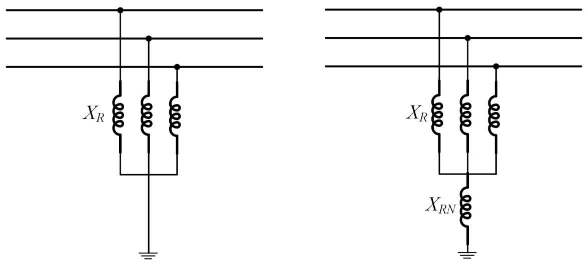

Fig. 10. (a) Three-reactor arrangement (b) Four-reactor arrangement.

positive and zero-sequence capacitive reactance can be wriiten as (23) and (24), respectively.

$$X_{C1}^{'} = \frac{X_R X_{C1}}{X_R - X_{C1}} \tag{23}$$

$$X_{C0}^{'} = \frac{X_R X_{C0}}{X_R - X_{C0}} \tag{24}$$

where X_{C1} and X_{C0} are the total positive and zero-sequence capacitive reactance of the transmission line; $X_{C1}^{'}$ and $X_{C0}^{'}$ are the effective positive and zero-sequence capacitive reactance of the transmission line; X_R is the total per phase inductive reactance of the reactors connected to the line the transmission line. For multiple reactor banks connected to transmission line X_R can be obtained by:

$$\frac{1}{X_R} = \frac{1}{X_{R1}} + \frac{1}{X_{R2}} + ... + \frac{1}{X_{Rk}} + ...$$

where X_{Rk} is the per phase inductive reactance of the k^{th} bank.

- Four reactor arrangement: In a four reactor arrangement, a fourth reactor with reactance X_{RN} is added in the neutral branch (see Figure 10 (b)), therefore, the positive-sequence reactance remains same as $X_{R1} = X_R$ while the zero-sequence reactance of the reactor arrangement becomes $X_{R0} = X_R + 3X_{RN}$. The equations for the effective positive and zero-sequence capacitive reactance for Four reactor arrangement can be wriiten as (25) and (26), respectively.

$$X_{C1}^{'} = \frac{X_R X_{C1}}{X_R - X_{C1}} \tag{25}$$

$$X_{C0}^{'} = \frac{(X_R + 3X_{RN}) X_{C0}}{X_R + 3X_{RN} - X_{C0}} \tag{26}$$

For multiple reactor banks having reactor in their neural branch X_{RN} can be obtained by:

$$\frac{1}{X_{RN}} = \frac{1}{X_{RN1}} + \frac{1}{X_{RN2}} + ... + \frac{1}{X_{RNk}} + ...$$

where X_{RNk} is the per phase inductive reactance of the k^{th} bank.

6.4 Short transmission line

A transmission line shorter than $80km$ is generally considered a short transmission line. The charging current in short transmission lines is in vicinity of 100A or lower and could generally be ignored as the fault current is relatively large. However, if the CT ratio is low such as 1000:5 or lower, then the steady state charging current will become around 10%. If it is required to use sensitive 87L settings to detect high impedance faults, then compensating the charging current should be considered. Figure 11 shows the charging current measured through different CT ratios (2000:5, 1500:5, and 600:5) for an $80km$, $500kV$ transmission line. It can be noted that when measured through CT with ratio 2000:5, the steady state charging current magnitude is approximately equal to $0.06pu$. Thus, in this case the charging current can be ignored while setting the minimum pick up of the 87L element. However, when the same charging current is measured though CT with ratio 600:5, the magnitude of the charging current becomes close to 0.18pu. In this case, it is advisable to compensate the charging current.

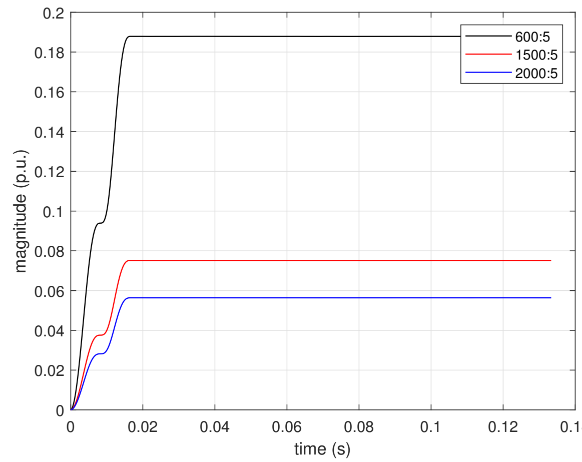

Fig. 11. Charging current of an $80km$, $500kV$ transmission line measured through different CT ratios.

7 Field Case

The event being discussed involved the mal-operation of line ground-current differential element 87LG element due to incorrect application of the charging current compensation. The system consisted of a 256km long 230kV transmission line with $X_{C1} = 810.0\Omega$, $X_{C0} = 1422.3\Omega$. A reactor bank in three-reactor arrangement with per phase reactance of 2645Ω was applied at each terminal of the transmission line, resulting in total per phase reactance (X_R) equal to 1322.5Ω. The CT ratio was 1250:1. Now, the effective positive-sequence capacitive reactance ($X_{C1}^{'}$) and zero-sequence capacitive reactance ($X_{C0}^{'}$) become , respectively as shown below:

$$X_{C1}^{'} = \frac{1322.5 \times 810.0}{1322.5 - 810.0} = 2090.2\Omega$$

$$X_{C0}^{'} = \frac{1322.5 \times 1422.3}{1322.5 - 1422.3} = -18847.6\Omega$$

The negative value of $X_{C0}^{'}$ signifies that the effective zero-sequence reactance is inductive in nature, while high magnitude of $X_{C0}^{'}$ signifies that even for the worse case scenario of a close-in external fault supplied by a weak source (leading to high magnitude of zero-sequence voltage), the zero-sequence charging current would be less than 5A or

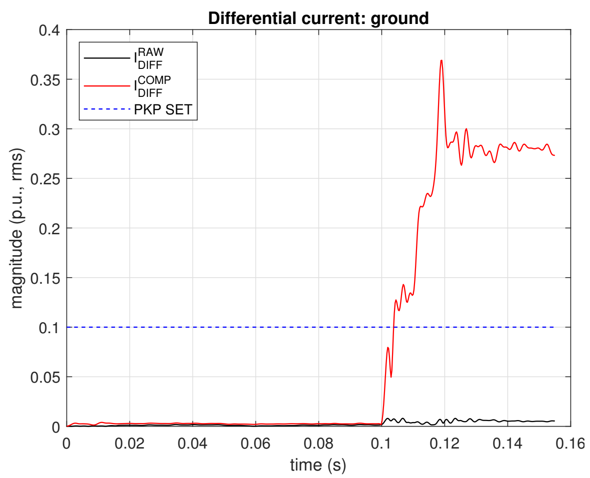

Fig. 12. Field Case of an external ACG fault: Raw and compensated ground differential current.

0.004pu. The minimum current pick-up setting for 87LG element was selected to be 125A or 0.1pu. Thus, leaving the safety margin of minimum pick-upof 87LG practically unaffected by the uncompensated zero-sequence charging current. Similarly, based on the values of $X_{C1}^{'}$, the charging current during normal operation would be approximately 63.5A or 0.05pu $\left(= \frac{63.5}{1250}\right)$ for phase line-current differential element (87L). The The minimum pick-up setting used for 87L element was 0.2pu or 250A. Therefore, it can be seen that a significant safety margin of about 0.15pu or 187.5A existed for 87L element too. Therefore, the charging current compensation was not necessary.

However, the user decided to enable the charging current compensation to further improve the safety margin. However, the relay did not allow for entering a negative value for the zero-sequence reactance setting ($X_{C0}^{'}$ is negative). The user selected the lowest positive value allowed to be entered for the zero-sequence reactance setting, thus, unintentionally applying a very large and incorrect capacitive charging current compensation. Note that the effective zero-sequence reactance is a large negative number which implies the charging current is inductive and very small. Now, when an external ACG fault occurred element 87LG mal-operated due to incorrect zero-sequence charging current compensation. Figure 12 shows the raw differential current (I_{DIFF}^{RAW}) without charging current compensation as well as the differential current due to erroneous charging current compensation (I_{DIFF}^{COMP}). It can be observed that I_{DIFF}^{COMP} magnitude rises upto 0.35pu and settles around 0.3pu, which is almost double the actual fault current flowing through the transmission line (i.e., $I_S \approx I_R \approx 0.15$pu). On the other hand the magnitude of I_{DIFF}^{RAW} remained very close to zero as expected due to the large value of $X_{C0}^{'}$. Thus it can be concluded that erroneous zero-sequence compensation resulted in the mal-operation of 87LG in this case.

Nevertheless, an argument can be made in this case that even if charging current compensation was not required in zero-sequence domain, there is still a standing charging current of approximately 0.05pu/63.5A on the phases, and enabling the charging current compensation can improve the security margin for 87L element. To accomplish this it is

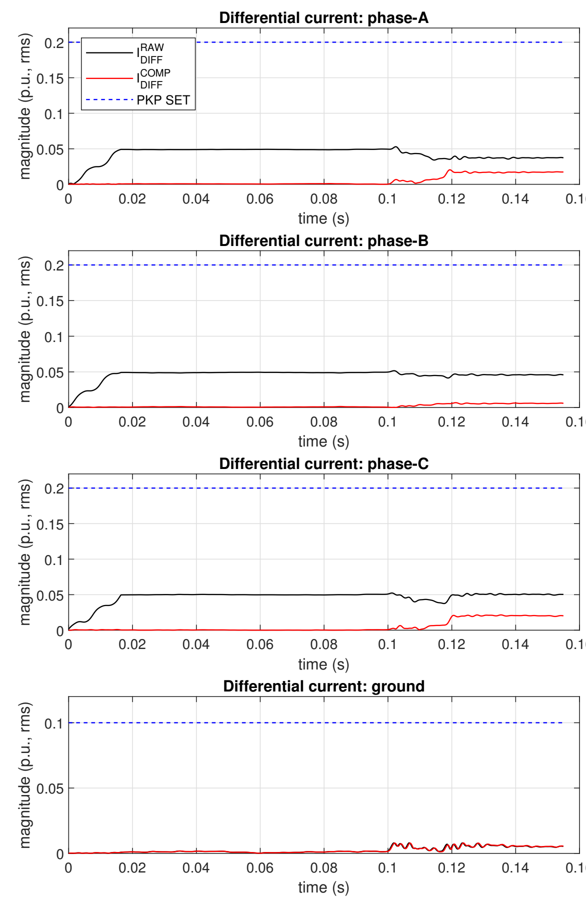

Fig. 13. Field Case of an external ACG fault: Raw and compensated differential current in phases-A, B, C and ground channel.

important that charging current compensation is effectively 'diasabled' by selecting a the highest possible number in the setting zero-sequence reactance, while the setting positive-sequence reactance is set to the above calculated value (2090.2Ω). This would ensure that a very small to negligible compensation would be applied to zero-sequence charging currents, while correct compensation is applied in positive and negative sequence domains. Note that significant safety margin of about 0.15pu/187.5A without applying charging current compensation as discussed earlier. Figure shows the differential current seen by 87L element in phases-A, B, C and ground channelby using the values 2090.2Ω and 65535Ω as positive-sequence and zero-sequence reactance settings, respectively. Note that in all phases I_{DIFF}^{COMP} is almost zero during prefault period and is almost half of I_{DIFF}^{RAW} during fault conditions. At the same time, the I_{DIFF}^{COMP} in ground channel remains close to Zero along with I_{DIFF}^{RAW}, thus highlighting the negligible zero-sequence charging current compensation.

8 Recommendations

Based on the above discussion and the field experience some considerations that should be taken in to account are explained below.

- Line zero-sequence capacitive reactance X_{C0} should always be higher than line positive-sequence capacitive reactance X_{C1}.

- If reactors are present and can be switched in or out, charging current needs to be estimated for both conditions to make a decision as to whether you should apply compensation or not.
- Steady state charging current can be estimated as $I_C = \frac{V_{LL}}{\sqrt(3) X_{C1}}$.
- If the pu charging current of the CT nominal in the worst configuration (when reactors are switched) is less than half of the 87L pickup setting, then charging current compensation is not needed, as there is enough security margin. For example, if the maximum charging current is 0.08pu, it is safe to not enable charging current compensation with an 87L pickup of 0.2pu or higher.
- Typically the 87L pickup setting should be at least 1 ½ times higher than the worst-case charging current when charging current compensation is enabled. When charging current compensation is disabled it has to be set to at least 2 ½ times the worst-case charging current or higher.
- Our recommendation for the 87L pickup setting above also applies to the ground differential function 87LG.
- The charging current compensation should not be aimed at completely eradicating the 'fictitious' differential current because other sources of error such as CT error, channel asymmetry, synchronization error, voltage transformer fuse failure (VTFF) condition can also lead to 'fictitious' differential current.
- Depending upon the reactor arrangement usage, if the result of any of the equations (23) to (26) produces a negative number for either $X_{C1}^{'}$ or $X_{C0}^{'}$ settings, this is an indication that line capacitive reactance has already been well-compensated for by shunt reactors. In this case, the charging current compensation must be disabled.

9 Conclusion

In this paper, the theory is presented which enables the analytical estimation of the line capacitance and hence line charging current. Various methods to overcome the challenge posed by the charging current for 87L element are presented. The voltage measurement-based charging current compensation method is explored in detail including when and how to apply voltage measurement based charging current compensation. The effects of charging current compensation on the safety margin of 87L element have been presented with help of a test system simulated in PSCAD. A detailed analysis of a field case is presented where the incorrect application of charging current compensation resulted in 87L mal-operation. The recommendations have been provided based on the field experience and simulation results about the successful application of charging current compensation.

Appendix A
Estimating charging current parameters from recorded waveforms

The Section 2 presented the method to estimate zero-sequence and positive sequence capacitances or reactances from the physical geometry of the conductor arrangements. It is actually possible to estimate zero-sequence and positive sequence capacitances or reactances by sing current and voltage waveforms. As discussed previously, if the charging current compensation is not applied then the charging current gets manifested as 'fictitious' differential current during normal operation and also in the case of an external faults. Therefore following equation would hold true for postive and zero-sequence charging currents:

$$I_{kS} + I_{kR} = \frac{V_{kS}}{2X_{Ck}} + \frac{V_{kR}}{2X_{Ck}}$$

where k attains value 0 for zero-sequence, 1 for positive sequence. Rearranging the above equation, the following equation is obtained:

$$X_{Ck} = \frac{V_{kS} + V_{kR}}{2(I_{kS} + I_{kR})} \tag{27}$$

For a loss less line the right hand side (R.H.S) of the equation (27) would be a purely an imaginary number but for a real lines it would have a relatively a negligible real part. Therefore, to remove the real part the equation (27) can be more appropriately written as:

$$X_{Ck} = imag\left(\frac{V_{kS} + V_{kR}}{2(I_{kS} + I_{kR})}\right) \tag{28}$$

X_{C1} can easily be obtained from equation (28) by using the voltage and currents from the normal operation of the system as positive sequence voltage and currents are available at normal operations. For obtaining X_{C0}, the voltage and currents from an external ground fault can be used because zero-sequence components appear only for the ground faults while the zero-sequence charging current appears as zero-sequence differential current for external faults only.

References

[1] J. D. Glover, M. S. Sarma, T. J. Overbye"Transmission Line Parameters," in Power System Analysis and Design, 5th ed. Stamford, USA: Cengage Learning, 2012, ch. 4, sec. 11, pp. 208

[2] https://www.pscad.com/webhelp/EMTDC/Transmission_Lines/The_PSCAD_Line_Constants_Program.htm

[3] Zhihan Xu, Ilia Voloh, Terrence Smith "87L Application on Long Transmission Line with Series Capacitor Banks and Shunt Reactors" *67th Annual Conference for Protective Relay Engineers*, College Station, TX, USA ,March 2014 2002.

Tirath Bains Tirath Bains received The B.E. degree in Electrical Engineering from Punjab Engineering College, Chandigarh, India in 2008. He completed his Master of Engineering Science and PhD degrees from The University of Western Ontario in 2014, and 2018, respectively. Since 2019 has been with GE as Lead Design Specialist in Research and Development at GE Grid Solutions, Markham, ON, Canada. His main research interest includes frequency-based and time-based protection and fault location algorithms, and high impedance fault detection algorithms.

Ilia Voloh received the Electrical Engineering degree from Ivanovo State Power University, Ivanovo, Russia. He is currently an Applications Engineering Manager with GE Grid Solutions, Markham, ON, Canada. He has authored and coauthored more than 60 papers presented at major North America Protective Relaying conferences. His areas of interest are advanced power system protection algorithms and advanced communications for protective relaying. He is a member of IEC TC95 committee and an active member of the main IEEE PSRC committee.

JC (Jacobus) Theron is Technical Applications Engineering Team Leader for Grid Automation division of GE Grid Solutions. He received the degree of Electrical and Electronic Engineer from the University of Johannesburg, South Africa in 1991. Mr. Theron has 30 years of engineering experience; 6 years with Eskom (South Africa) as Protection / Control and Metering Engineer, 17 years with GE Multilin (Canada) as Technical Applications Engineer/ Product / Technical support / Protective Relaying Consultant/Protection and Systems Engineer leading the Project and Consulting Engineering team and as Product Manager, 2 years with Alstom T&D (USA) as Senior Systems Engineer and 5 years with Hydro One as Operations Assessment Engineer / P&C Technical Services Manager. He specializes in transmission, distribution, bus and rotating machines protection applications support and Fast Load Shed Systems, system designs and transient system testing. He is member of IEEE.

Hebert Marchi graduated in Electrical Engineering from the Federal University of São João del-Rei, Brazil. Hebert specializes in protection and control systems, and currently working in the implementation of transmission projects in Brazil.